About Minimal Surfaces

DISCOVERY AND PHYSICAL INTERPRETATION.

The question *which surfaces locally minimize area* led Lagrange in 1760 to the minimal surface equation for graphs. By 1765 Meusnier had found that a geometric interpretation of this equation is: *the mean curvature of the surface vanishes.* He discovered that the catenoid and the helicoid are nonplanar examples. It took until 1835 for the next examples to appear, discovered by Scherk; his doubly periodic surface is a graph over the black squares of a checkerboard tesselation of the plane and his singly periodic surface is nowadays viewed as a desingularization of two orthogonally intersecting planes. In the following years complex analysis developed and by 1865 many examples were known through the efforts of Riemann, Weierstraß, Enneper and in particular Schwarz.

Also in that period Plateau had made careful experiments with soap films. He convinced people that soap films were a perfect physical realization of minimal surfaces, and he convinced mathematicians that they should solve *Plateau's Problem,* i.e. prove that every continuous injective closed curve in $\mathbb{R}^3$ spans a minimal surface. This problem was solved in 1932 by Douglas and independently by Rado. On the way to this solution mathematicians had learnt a lot about nonlinear elliptic partial differential equations.

In particular the importance of the *maximum principle* had become clear, it implies for example that every compact minimal surface is contained in the convex hull of its boundary and that boundary value problems are well posed for the minimal surface equation.

On the other hand, although the Cauchy-Kowalewski theorem allows to solve locally initial value problems with analytic data, there is no continuous dependence on the data and no hope to obtain complete immersed examples with this method. — But, already Weierstraß had established the close connection of minimal surfaces with complex analysis. In particular: the spherical Gauss map composed with stereographic projection is locally a holomorphic function $G : M^2 \to \mathbb{C}$. In terms of the 90° rotation of each tangent space of the minimal surface M^2 holomorphicity has the following intuitive interpretation: for each $v \in TM^2$ we have the following version of the Cauchy-Riemann equations

$$dG(\mathbb{R}90 \circ v) = i \cdot dG(v).$$

Moreover, the three component functions of the immersion $(F^1, F^2, F^3) : M^2 \to \mathbb{R}^3$ are, locally, the real parts of holomorphic functions because the differential forms $\omega^j := -dF^j \circ \mathbb{R}90$ are closed for surfaces with mean curvature zero (Meusnier's above interpretation of "minimal"). This fact establishes the Weierstraß representation:

> Let G be the holomorphic Gauss map and $dh := dF^3 - i \cdot dF^3 \circ \mathbb{R}90$ the (holomorphic) complex-

ification of the differential of the height function F^3 then

$$(F^1, F^2, F^3) = \text{Re} \int \left(\frac{1}{2}(\frac{1}{G} - G), \frac{i}{2}(\frac{1}{G} + G), 1 \right) dh.$$

The examples of the second half of the 19$^{\text{th}}$ century were made with this representation. But results, achieved by 1960 by Huber and Osserman show, that *all* minimal surfaces of a certain kind can be obtained by a global application of this representation, namely:

Complete, immersed minimal surfaces of finite total curvature can be conformally compactified by closing finitely many punctures; moreover, the Weierstraß data G, dh extend *meromorphically* to this *compact Riemann surface.*

The wealth of examples, discovered since about 1980, rely on this theorem. To understand these examples better we note the first and second fundamental forms (Riemannian metric and, if $|v| = 1$, normal curvature)

$$I(v, v) = \frac{1}{4}(\frac{1}{|G|} + |G|)^2 |dh(v)|^2$$

$$II(v, v) = \text{Re}\frac{dG(v)}{G} dh(v).$$

The points p on the Riemann surface which are poles of dh do not correspond to points on the minimal surface. Every

(differentiable) curve which runs into such a *puncture p* has infinite length on the minimal surface. The same is true if G has a zero or pole of higher order than the vanishing order of dh. If these orders are the same then we simply have a point with vertical normal on the minimal surface. And at points where the vanishing order of dh is larger, the metric becomes singular and the minimal surface has a so called *branch point*, it is no longer an immersion.

VISUALIZATION OF MINIMAL SURFACES.

The Weierstraß representation allows to write down a number of simple minimal surfaces which can be visualized like any other surface for which an explicit parametrization is given. Our parameter lines come from polar coordinates with centers $\{0, \infty\}$ or $\{1, +1\}$. Note that the zeros and poles of G, dh fit together so that no branch points occur and so that the minimal surfaces are complete on the punctured spheres mentioned in each case. The surfaces are of finite total curvature, since the Gauss map is meromorphic, i.e., its image covers the Riemann sphere a finite number of times.

FIRST EXAMPLES,
defined on $\mathbb{C}$ or $\mathbb{C} \setminus \{0\}$ or $\mathbb{S}^2 \setminus \{1, -1\}$:

Enneper Surface:
$$z \in \mathbb{C}, \ G(z) := z, \ dh := zdz$$

Polynomial Enneper:
$$z \in \mathbb{C}, \ G(z) := P(z), \ dh := P(z)dz$$

4

Rational Enneper:

$$z \in \mathbb{C}, \ G(z) := P(z)/Q(z), \ dh := P(z)Q(z)dz$$

P and Q are polynomials without common zeros.

Vertical Catenoid:

$$z \in \mathbb{C} \setminus \{0\}, \ G(z) := z, \ dh := dz/z,$$
$$\text{or } G(z) := 1/z$$

Helicoid:

$$z \in \mathbb{C}, \ G(z) := \exp(z), \ dh := \mathbf{i}dz = \mathbf{i}\frac{dG}{G}$$

Helicoid:

$$z \in \mathbb{C} \setminus \{0\}, \ G(z) := z, \ dh := \mathbf{i}dz/z$$

Planar to Enneper:

$$z \in \mathbb{C} \setminus \{0\}, \ G(z) := z^{k+1}, \ dh := z^{k-1}dz$$

Wavy Catenoid:

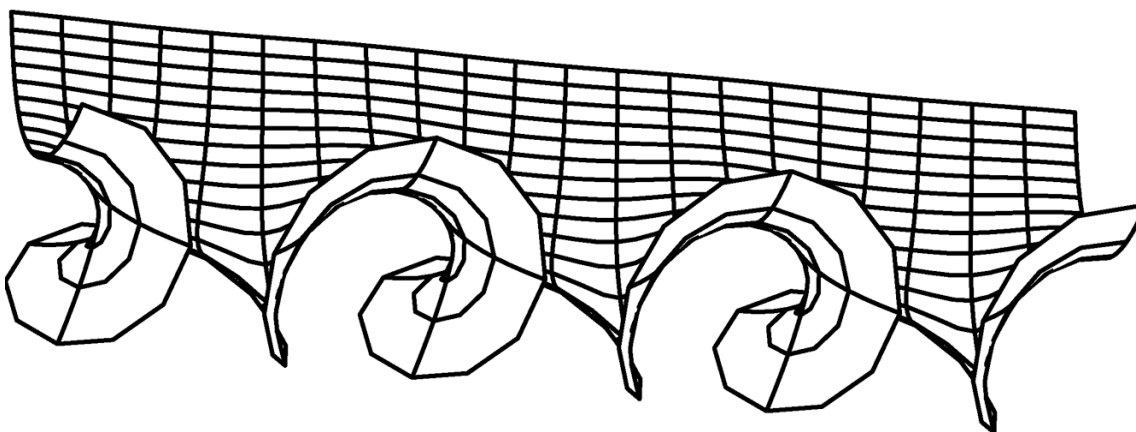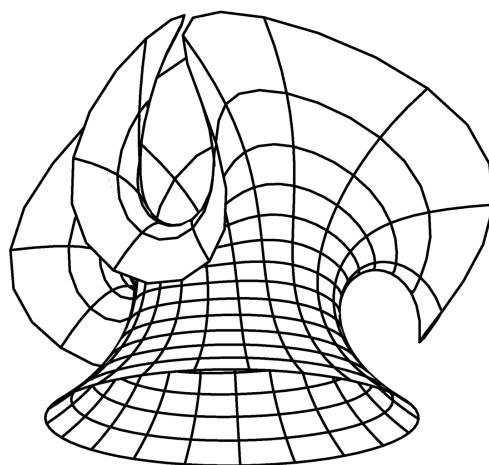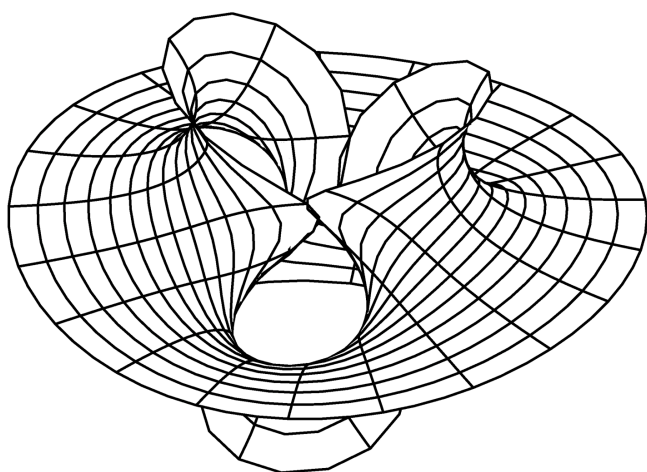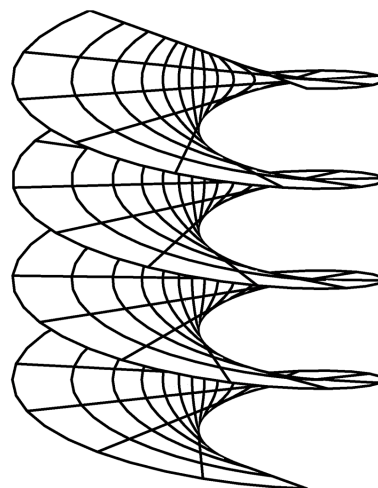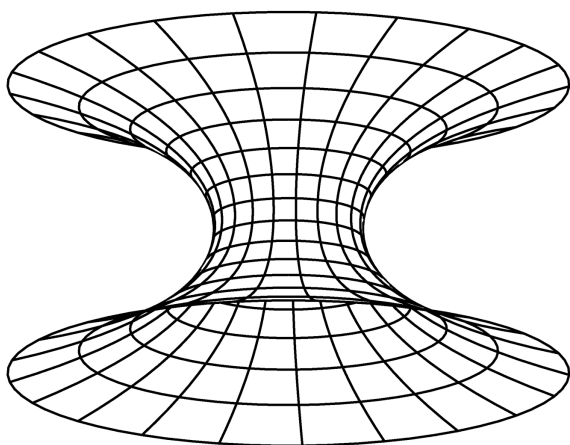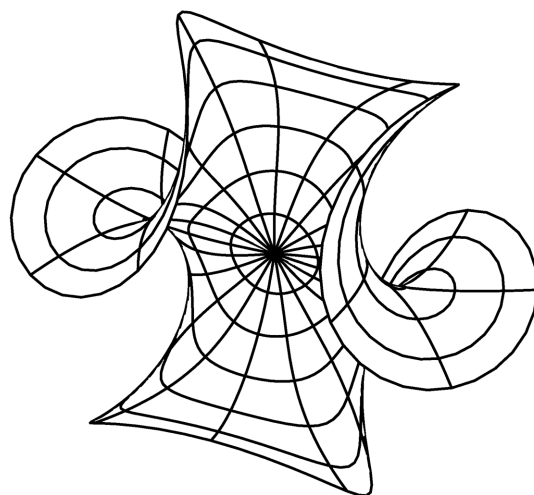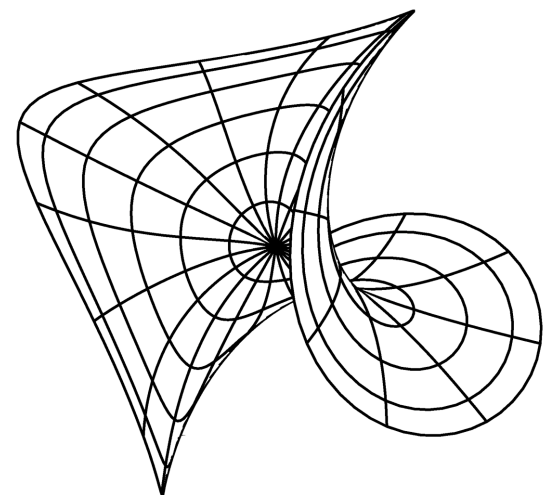$$z \in \mathbb{C} \setminus \{0\}, \ G(z) := (1 + \epsilon \cdot z^k)/z, \ dh := G(z)dz$$

Wavy Plane:

$$z \in \mathbb{C} \setminus \{0\}, \ G(z) := z, \ dh := dz$$

Horizontal Catenoid:

$$z \in \mathbb{S}^2 \setminus \{1, -1\}, \ G(z) := z, \ dh := \frac{dz/z}{(z - 1/z)^2}.$$

All of these simple minimal surfaces have *symmetries*: (i) straight lines on a minimal surface allow 180° rotations of the minimal surface into itsself, and (ii) planar geodesics on a minimal surface allow reflection (in the plane of the geodesic) of the minimal surface into itsself. Since these symmetries become more important for understanding more complicated surfaces one should learn how to recognize them. The straight lines are geodesics with normal curvature $II(c', c') = 0$ or $dG(c')/G \cdot dh(c') \in \mathbf{i} \cdot \mathbb{R}$. In the present context we recognize geodesics as fixed point sets of isometric involutions. The formula for the first fundamental form is so simple that one can easily see in all of these examples that the expected symmetry indeed does not change the Riemannian arc length of curves. To recognize the planar geodesics note that a geodesic on a surface is planar if it is also a principal curvature line; in addition to seeing it as the fixed point set of a length preserving involution we therefore only need to check $dG(c')/G \cdot dh(c') \in \mathbb{R}$, which is also easy in these examples.

In 3D-XplorMath one can easily change (in the Settings Menu) the range of the parametrization and also the symmetry of the surface. We recommend that the surfaces are looked at from far away when a large range for the parametrization is chosen. We also recommend to look at the default morphs of WavyEnneper and WavyCatenoid since it is quite surprising how suddenly the perturbation becomes visible. This should be taken as an illustration that the initial value problem for minimal surfaces is highly

unstable, it is *ill posed* and no numerical solution is possible.

MORE COMPLICATED SPHERICAL EXAMPLES.

The sudden increase of the interest in minimal surfaces after 1980 was largely caused by the discovery of a quite unexpected embedded finite total curvature minimal surface by Costa with embeddedness discovered and proved by Hoffman-Meeks. We are not yet close to such an example because of the following

Theorem of Lopez-Ros. An embedded, minimal, finite total curvature punctured sphere is a plane or a catenoid.

To practise using the Weierstraß representation we therefore have to be content with a few immersed punctured spheres. We want to learn *how to see the Gauss map* when one looks at the picture of such a minimal surface. The main fact to use is: a meromorphic function on a compact Riemann surface is determined up to a constant factor by its zeros and poles. In the case of the Jorge-Meeks k-noids one clearly sees a k-punctured sphere with a horizontal symmetry plane. One observes only two points with vertical normal, one up, one down. The qualitative behaviour of the Gauss map along the horizontal symmetry line suggests a mapping degree $k - 1$. This leaves no choice but $G(z) = z^{k-1}$. If we look back at the very simple examples then we can observe that, at a catenoid like puncture, either $G dh$ or dh/G has precisely a double pole. This determines the dh below up to a constant factor.

The next two examples, the 4-noid with orthogonal ends of different size, and the double Enneper, have a quite different appearance, but they have the same Gauss map. The vertical points are symmetric with respect to the origin and symmetric with respect to the unit circle, and the degree of the Gauss map is three; this determines the Blaschke product expression below. In the case of the 4-noid we need to create the four catenoid ends with double poles of dh and we need to compensate the simple zeros and poles of G by simple zeros of dh; then, if we also treat zero and infinity symmetrically, the expression below is forced. In the case of the double Enneper surface we just need to compensate the simple zeros and poles of G (outside $0, \infty$); symmetric treatment of $0, \infty$ gives the dh below (except for a constant factor).

The last example illustrates in which way attempted counter examples to the Lopez-Ros theorem fail. A residue computation for the Weierstraß integrands shows that closed curves around the punctures ± 1 on the sphere are *not* closed curves on the minimal surface, if we want all limit normals to be vertical. It is easy to close this so called *period* when one allows tilted catenoid ends, but, as one decreases the tilt, the distance between the half catenoids increases, and they intersect the planar middle end if one computes the surface far enough towards the punctures.

The k-noids of Jorge-Meeks:

$$z \in \mathbb{S}^2 \setminus \{e^{2\pi \mathbf{i} \cdot l/k};\ 0 \leq l < k\},$$

$$G(z) := z^{k-1}, \quad dh := (z^k + z^{-k} - 2)^{-1} \cdot dz/z.$$

4-noids with two different orthogonal ends:

$$z \in \mathbb{C} \setminus \{0, -1, +1\}, \quad G(z) := z \cdot \frac{z-r}{1-rz} \cdot \frac{z+r}{1+rz},$$

$$dh := \left(1 - \frac{z^2+z^{-2}}{r^2+r^{-2}}\right) \cdot (z^2 - z^{-2})^{-2} \cdot dz/z.$$

Two Enneper ends joined by a catenoidal neck:

$$z \in \mathbb{C} \setminus \{0\},$$

$$G(z) := z \cdot \frac{z-r}{1-rz} \cdot \frac{z+r}{1+rz}, \quad dh := \left(1 - \frac{z^2+z^{-2}}{r^2+r^{-2}}\right) \cdot dz/z.$$

Three punctures, period closes for tilted ends:

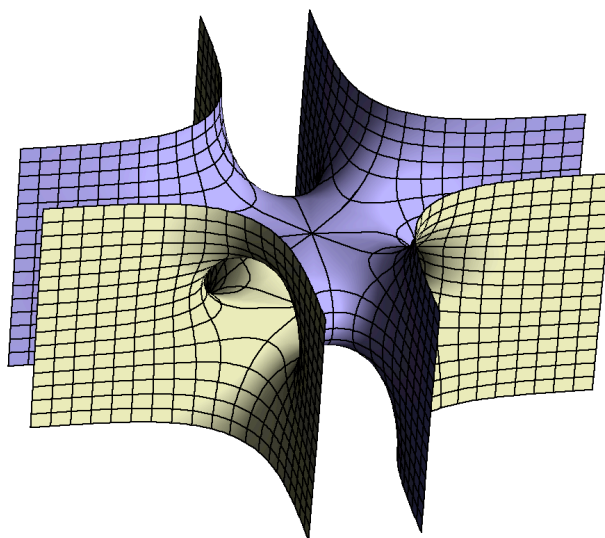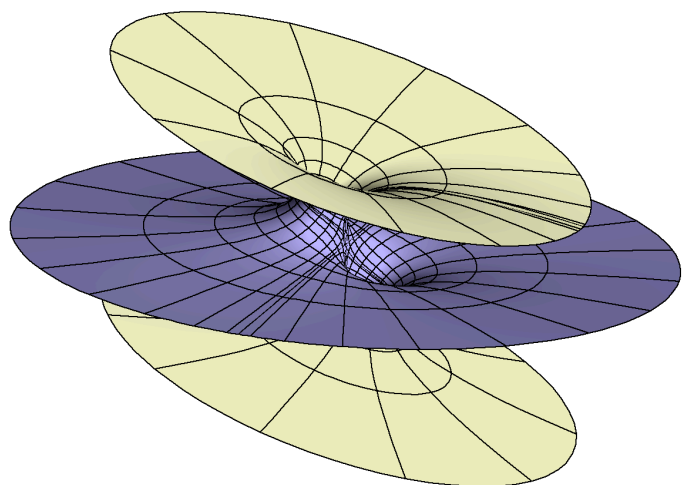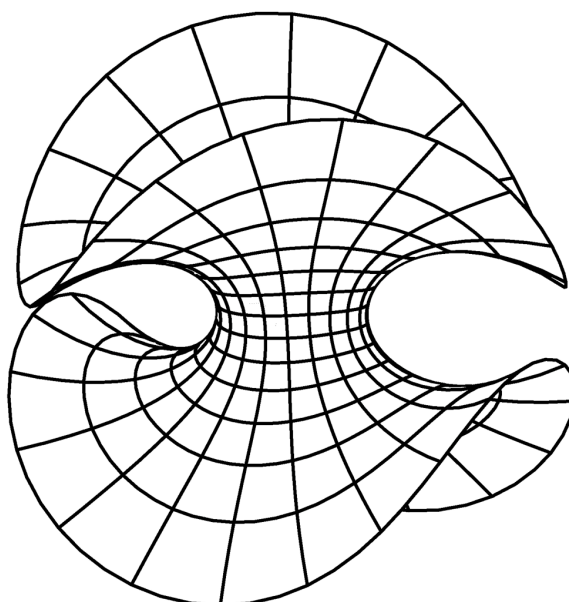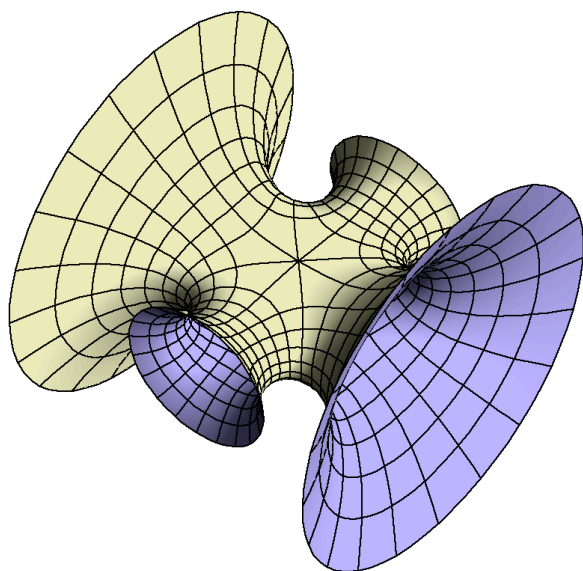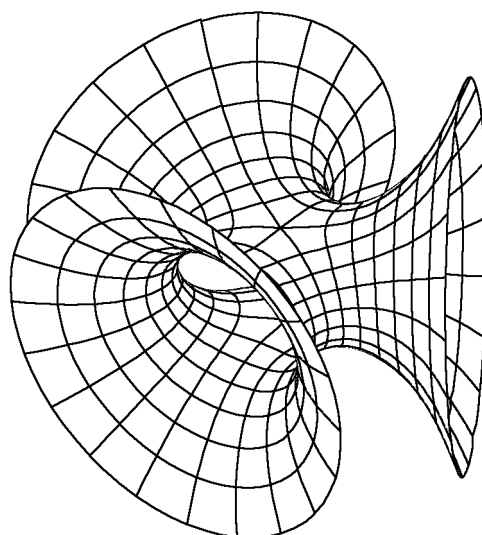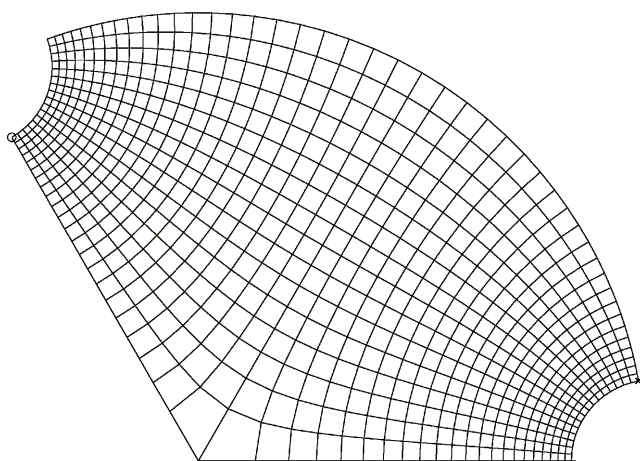$$z \in \mathbb{C} \setminus \{-1, +1\},$$

$$G(z) := \rho(z^2 - r^2), \quad dh := \frac{z^2-r^2}{(z^2-1)^2} dz.$$

Observe that the zeros and poles of the Gauss map which are not in the list of punctures are compensated by zeros of dh. At the embedded ends, Gdh or dh/G have a double pole and at the Enneper ends they have higher order poles. — In this list we do not have simple poles of Gdh and dh/G. If this happens then the Weierstraß integral behaves similar to $\int dz/z$: the unit disk, punctured at 0, is mapped by log to an infinite number of half strips parallel to the negative real axis and of width 2π. Similarly, the Weierstraß integral produces *simply periodic embedded minimal surfaces* parametrized by punctured spheres.

Generalized Scherk Saddle Towers:

$$z \in \mathbb{S}^2 \setminus \{e^{\pm\phi} \cdot e^{2\pi \mathbf{i} \cdot l/k}; \ 0 \leq l < k\},$$

$$G(z) := z^{k-1}, \quad dh := (z^k + z^{-k} - 2\cos k\phi)^{-1} \cdot dz/z.$$

As in the simpler examples, observe that the symmetry lines can be seen from the Weierstraß data. We also note that at this point an important decision has to be made. If one represents the surfaces, as in all our examples, with parameter lines then each surface requires a special effort so that the parameter lines on the one hand support the complex analytic background of the minimal surface and on the other hand suggest correctly how one should imagine how the surface extends beyond what the picture shows. In 3D-XplorMath this individual approach has been taken. The other option is to spend considerably more general effort by writing software which will create a suitable triangulation of the domain. David and Jim Hoffman have such a program running. It requires much less individual work to compute another minimal surface but it is harder to illustrate the complex analysis background of the computed minimal surface.

The family of singly periodic embedded minimal surfaces which resemble the above generalized Scherk Saddle towers is much larger than the above explicit formulas suggest. So far we have only talked about the real part of the Weierstraß integral. In fact, a 1-parameter ("associate") family of isometric (and in general not congruent) minimal surfaces are given by this integral because dh can be changed by the factor $\exp(-2\pi i \varphi)$. In particular, the imaginary part of the Weierstraß integral is the "conjugate" minimal surface. In the case of the generalized Scherk saddle towers we have that the conjugate minimal immersion maps the

unit disk (with the punctures on the boundary) to a graph over a convex polygon; its edge lengths all agree. The minimal graph has over each edge the boundary value $+\infty$ or $-\infty$, alternatingly. — Jenkins-Serrin proved the converse: every such infinite boundary value problem has a graph solution, a minimal disk whose conjugate minimal surface is the fundamental piece of an embedded singly periodic saddle tower.

Having seen a good collection of minimal surfaces parametrized by punctured spheres we now turn to minimal surfaces parametrized by other Riemann surfaces.

H.K.

Half-Catenoids and Weierstrass' Representation

In this text we try to explain, starting from scratch, minimal surfaces parametrized by tori.

We assume from complex analysis roughly the following: The complex logarithm, $\log(z)$, is a multivalued function with derivative $\log'(z) = 1/z$. One can compute the logarithm by integrating the differential form dz/z along a curve $c : [0,1] \mapsto \mathbb{C}$ with $c(0) = 1$, $c(1) = z$:

$$\log(z) := \int_c \frac{1}{\zeta} d\zeta := \int_0^1 \frac{c'(t)}{c(t)} dt$$

Of course, the integration path c has to avoid 0. Therefore one can reach z from 1 in many ways. A basic property of such complex line integrals is that their value does not change if the path is deformed, but with fixed endpoints. Two paths which wind around 0 a different number of times cannot be deformed into each other and, indeed, the values of the integrals along the two paths differ by an integer multiple of $2\pi i$. This number, the value of the integral from 1 once around 0 and back to 1, is called *the period of the differential form dz/z at its singularity* 0. The real part of this integral has no period, we have: $\operatorname{Re}(\log(z)) = \log|z|$ for all paths from 1 to z.

Instead of integrating one differential form we can integrate three, so that the real part of such an integral maps (a piece of) the complex plane into $\mathbb{R}^3$. The image is a surface without singularities if the integrand is never $(0,0,0)$. If

the integrand has singularities, the integration path has to avoid them and there may be periods. This means that the integral gives us not just one image of its domain, but a periodic repetition of one image. The obtained surfaces are in general not minimal surfaces, but one is close to them.

Weierstrass derived the following representation:

Let $D \subset \mathbb{C}$ be some domain, $g : D \mapsto \mathbb{C}$ a holomorphic function and dh a holomorphic 1-form on D. Then:

$$F_\varphi(z) := \mathrm{Re} \left(e^{i\varphi} \cdot \int_*^z \big(\tfrac{1}{2}(1/g - g), \tfrac{i}{2}(1/g + g), 1\big) dh \right)$$

maps, for each φ, D to a minimal surface piece in $\mathbb{R}^3$.

The length of the image of curves c in D can be computed with the Riemannian metric:

$$ds = \frac{1}{2}\Big(|g(c(t))| + \frac{1}{|g(c(t))|}\Big)|dh(c'(t))dt|.$$

Beyond the metric we do not discuss the differential geometry here. See "About Minimal Surfaces" for a derivation of the above Weierstrass representation that starts from the minimal surface definition. Instead we discuss Weierstrass' formula.

Since the Riemannian metric does not depend on the parameter φ the above surface pieces are all isometric to each other (almost never congruent). This is a rare phenomenon in surface theory. – Zeros of the differential form dh lead to

zeros of dF_φ. Such singularities are called *branch points* of the minimal surface. The Riemannian metric shows that they can be avoided if the function g has a zero or a pole of the same order as the zero of dh. See the Henneberg surface to view branch points.

Stereographic projection between the Gaussian plane $\mathbb{C}$ and the Riemann sphere $\mathbb{S}^2$ is an important tool in complex analysis. Composition of the function g with stereographic projection is

$$\vec{N}(z) := \left(2\mathrm{Re}\,(g), 2\mathrm{Im}\,(g), |g|^2 - 1\right)/(|g|^2 + 1) \in \mathbb{S}^2.$$

This vector is orthogonal to the integrand of the Weierstrass formula and therefore a unit normal vector field of the surface. The Weierstrass representation is therefore built from a unit normal field and the differential of the height function. The functions $g, \vec{N}$ are both called *Gauss map* of the surface. – We mention that a surface is minimal if its Gauss map $\vec{N}$ is anti-conformal. The 'anti' comes in because a minimal surface has Gauss curvature $K \leq 0$. Of the two choices for stereographic projection we used the anticonformal one.

One of the simplest examples, the catenoid and its conjugate, the helicoid, are obtained from the following Weierstrass data:

$$D := \mathbb{C} \setminus \{0\}, \ g(z) = z, \ dh = \frac{dz}{z}.$$

The 3rd component of the Weierstrass integrand has the imaginary period of dz/z which we discussed. The first and

second components have no periods because the singular terms dz/z^2 have the antiderivative $-1/z$ (so that the period integrals around the singularity vanish). If we set the *associate family* parameter $\varphi = 0$ we get a surface without period, a conformal immersion of $\mathbb{C} \setminus \{0\}$, the catenoid. If we set $\varphi = \pi/2$ we obtain a surface with vertical translation period, an immersion of the universal covering of $\mathbb{C} \setminus \{0\}$, the helicoid.

Remark. If one wants to visualize a surface one usually needs to choose parameter lines. In case of the catenoid: Only if one chooses polar coordinates around $\{0, \infty\}$, does the catenoid look familiar. For all other choices one can hardly recognize it. With the good choice, the parameter lines are the principal curvature lines. I believe these lines give the eye the best clues to imagine the surface correctly in space.

As in the case of the catenoid: Interesting Weierstrass data have isolated singularities, usually zeros or poles. The following summary helps to find interesting examples:
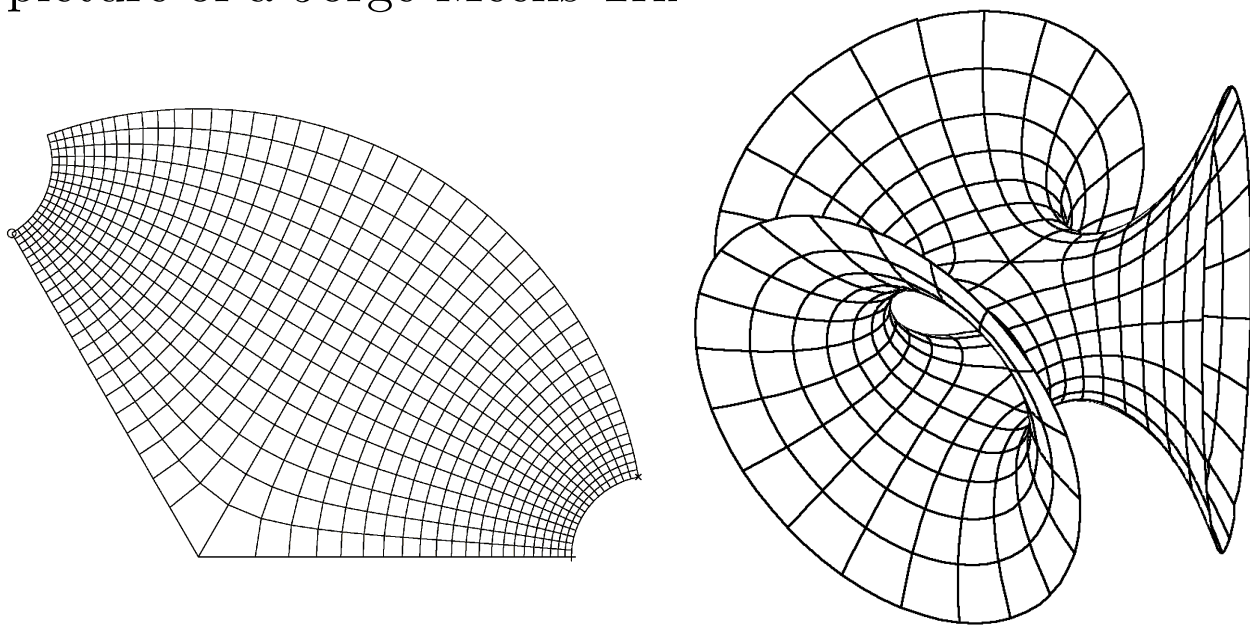
Poles of dh are never on the surface and lines into the puncture are infinitely long on the surface.

Zeros of dh have to be canceled by either a zero or else a pole of g which have the same orders as the zeros of dh.

If a puncture is to be a half-catenoid, then the Gauss map g must be single valued at the puncture. Furthermore, either $g \cdot dh$ or else dh/g must have a double pole (as in the case of the catenoid).

Let us try to find the Weierstrass data for the following
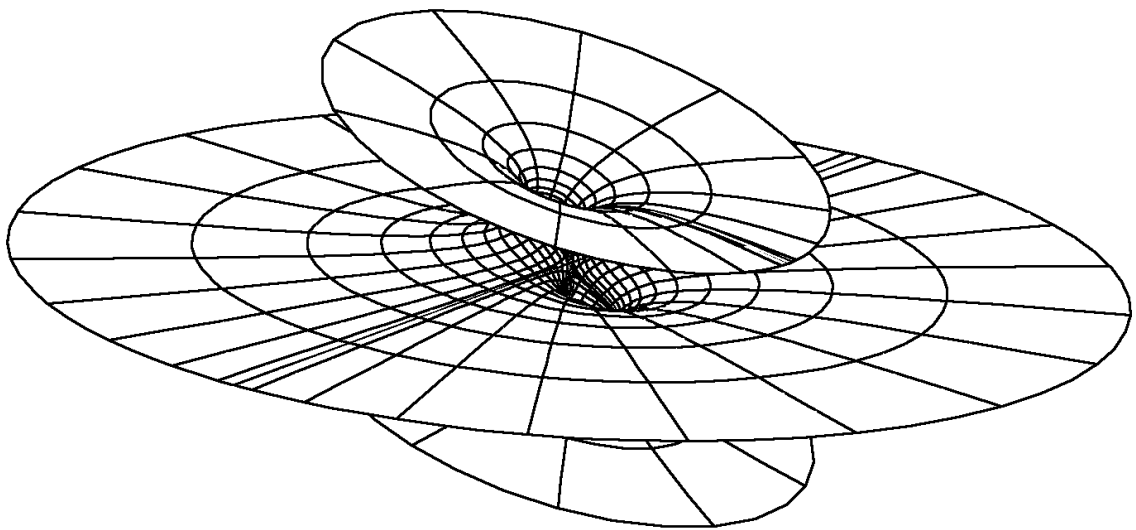
picture of a Jorge-Meeks Trinoid.

We have learnt from the catenoid that the huge opening
of a catenoid is conformaly only a puncture, just one *point*
missing. The picture therefore shows a sphere with three
punctures, say on the equator. With this orientation there
are just two points with vertical normals, one pointing
up, the other down. This implies that the Gauss map
is some power of z. Along the equator we find, for each
half-catenoid, one more normal which points in the same
direction as its limiting normal. The degree of g is there-
fore 2, hence $g(z) = const \cdot z^2$, and $|const| = 1$ to have
horizontal normals along the equator. Next dh. It needs
double zeros at $0, \infty$ to cancel the double zero and pole of
g and it needs double poles at the third roots of unity to
create the half-catenoids. Since dz/z is, up to sign, invari-
ant under inversion $z \mapsto 1/z$, we write dh as a multiple of
dz/z (which has simple poles at $0, \infty$).

This gives the Weierstrass data of the trinoid:

$$g(z) := z^2, \quad dh = \frac{z^3}{(z^3 - 1)^2} \cdot \frac{dz}{z}$$

To get good parameter lines, i.e. polar coordinates near the punctures, we use for one third of the unit disk the grid shown to the left of the trinoid. Closed parameter lines ('circles') in the domain around a puncture are mapped to closed curves in space since two orthogonal planes of symmetry cut the space curves into four congruent arcs.

Next let us grow two half-catenoids out of the plane as follows:

Observe that the limiting normals of the two half-catenoids point in the same direction, but not quite opposite to the normal of the plane. On each half-catenoid one can locate a finite point where the normal is opposite to the normal of the plane. The Gauss map has two simple zeros at these points, say at ± 1, and a double pole at ∞. Therefore we found $g(z) = c \cdot (z - 1)(z + 1)$. The zeros of g have to be

canceled by simple zeros of *dh* and *dh* needs double poles at points $\pm r$ to create half-catenoids there.

This gives us a 2-parameter family of Weierstrass data:

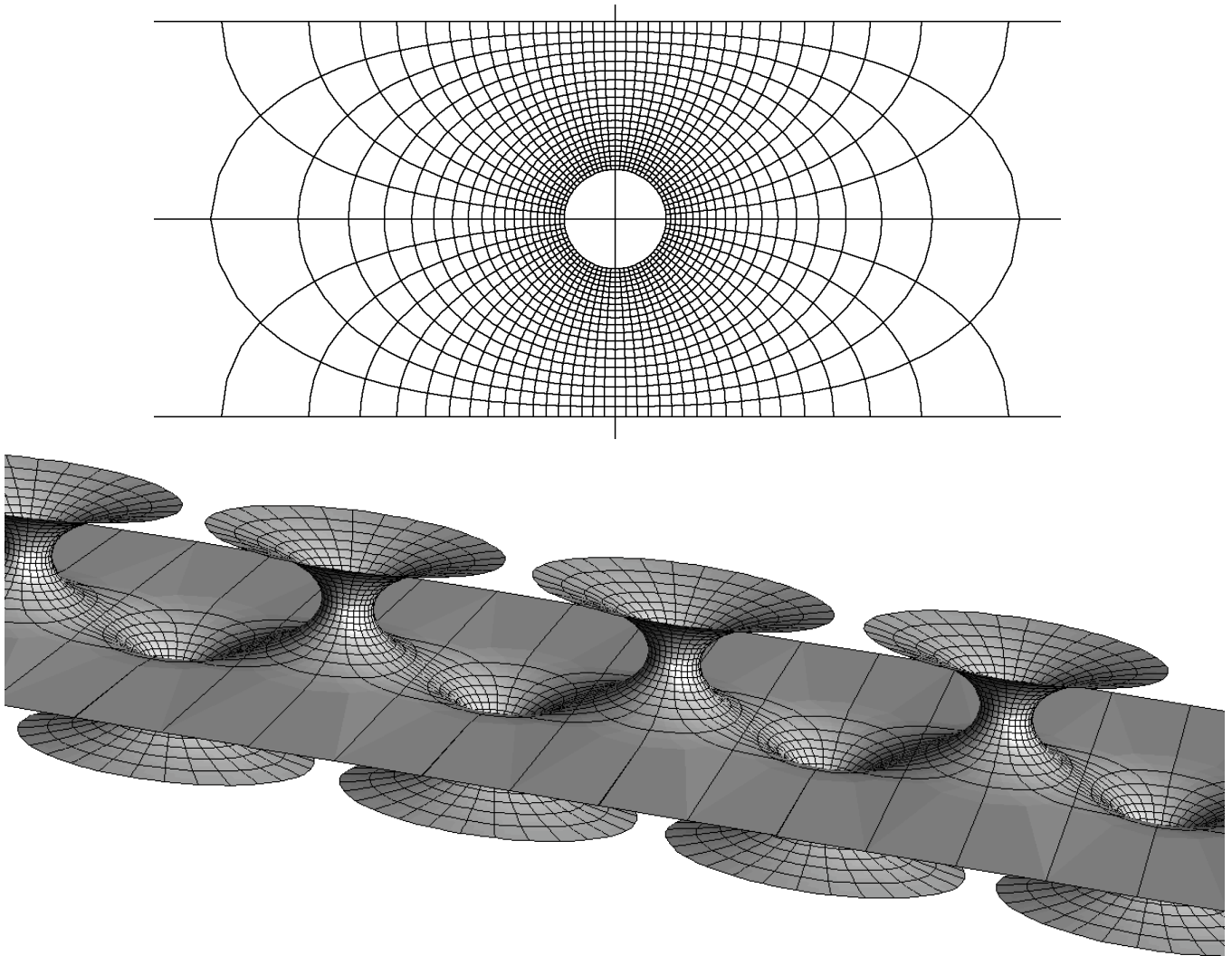$$g(z) := c \cdot (z - 1)(z + 1), \;\; dh := \frac{z^2 - 1}{(z^2 - r^2)^2} \cdot dz.$$

In this case there is only one vertical symmetry plane cutting the half-catenoids. Therefore closed curves around the punctures are not by symmetry mapped to closed curves in space, a period orthogonal to this plane can occur. The parameter c can be used to make this period vanish, for each $r > 1$. As r approaches 1 the two half-catenoids move further and further apart. In other words: one cannot grow two half-catenoids with limiting normals orthogonal to the plane. The half-catenoids will therefore always intersect the plane so that all these surfaces are only immersed, none is embedded.

It is however possible to grow infinitely many equidistant half catenoids out of the plane such that all these half-catenoids have the same limiting normal and this normal is opposite to the normal of the plane. The straight symmetry line between neighboring half-catenoids – which was present in the previous example – continues to exist. Therefore one needs to compute the surface only in a strip between neighboring symmetry lines.

The Weierstrass data are easy to guess:

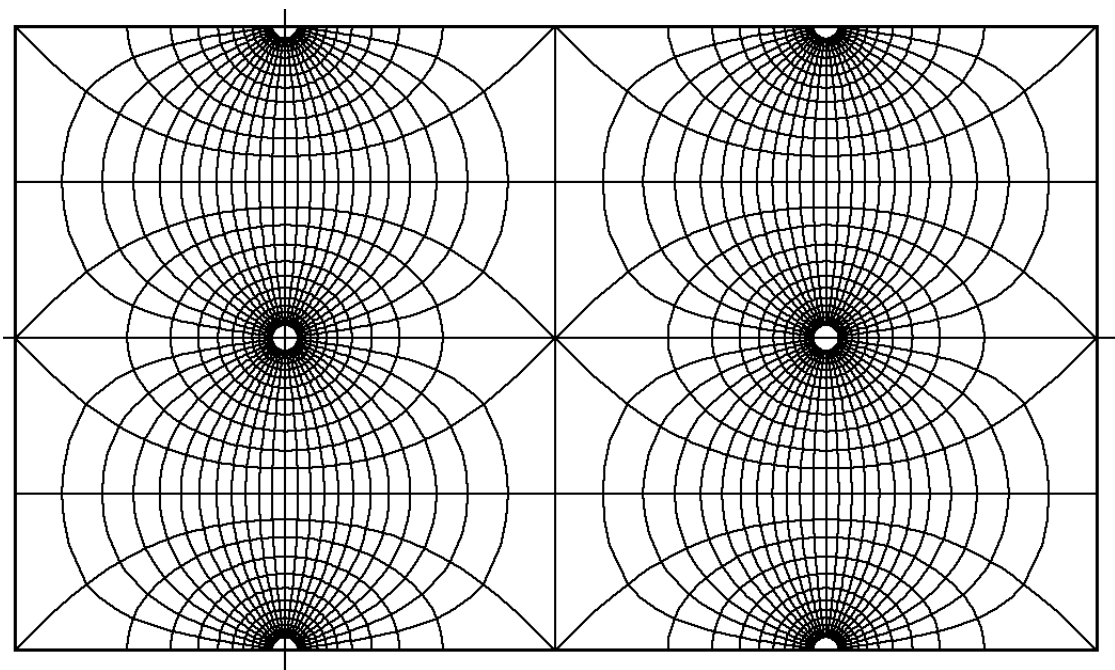$$g(z) := c \cdot \sin(z), \;\; dh := \frac{dz}{\sin(z)},$$

where $c \in \mathbb{R}$ controls the size of the half-catenoids relative to their distance. It is more complicated to get polar coordinates in a strip. Here is the result:

While sin has in the plane an essential singularity at ∞, in the strip there is convergence. The strip with edges identified is a cylinder with two half-catenoid punctures – or a sphere with four punctures, the two half-catenoids and the two ends of the flat strip. This last point of view suggests rational Weierstrass data:

$$g(z) := c \cdot (z - 1/z), \ \ dh := \frac{1}{z - 1/z} \cdot \frac{dz}{z}, \ \ c \in \mathbb{R}.$$

Beyond the singly periodic trigonometric functions one has the doubly periodic meromorphic elliptic functions. 'Doubly periodic' means that we have two independent translational symmetries. The group of translational symmetries is called a lattice Γ in $\mathbb{C}$. Each lattice has a parallelogram as fundamental domain and identification of opposite edges makes the parallelogram into a torus. Meromorphic elliptic functions can therefore be viewed as maps from tori to the Riemann sphere. We visualize an elliptic function (denoted J_F in 3D-XplorMath)by drawing the preimage on the torus of the usual polar grid on the Riemann sphere:
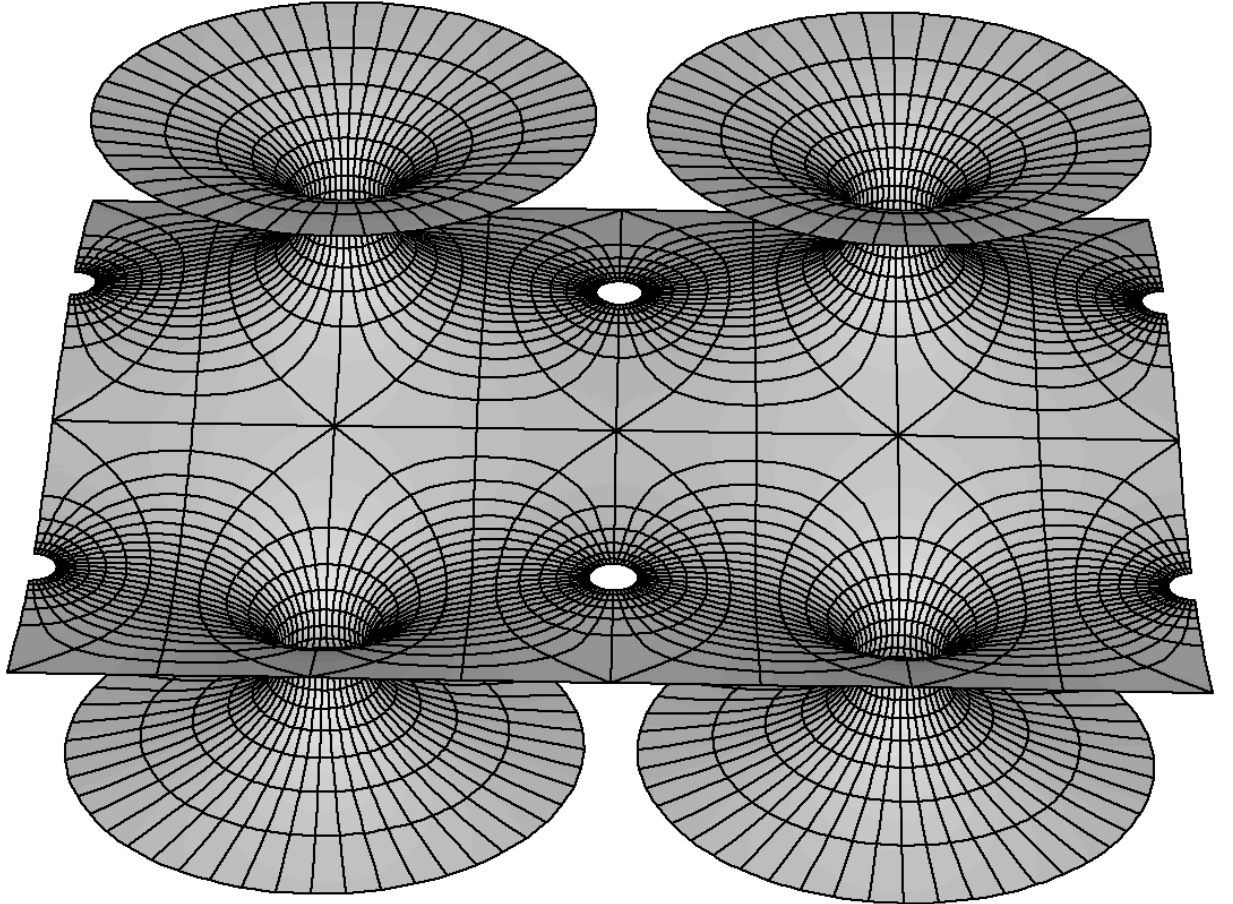

The two coordinate centers in the middle are zeros of the function, the two centers on the (identified) boundary are poles. The rectangles around the polar centers (made of symmetry lines of the picture) are preimages of the unit circle.

If we use this elliptic function in the same way as we used

the sin-function before:

$$g(z) := c \cdot J\_F(z), \quad dh := \frac{dz}{J\_F(z)},$$

then we obtain the following doubly periodic minimal surface:

The picture shows two copies of a fundamental domain for the translational symmetries. The half-catenoids are at the zeros of the function J_F. At its poles are the zeros of dh and these cancel the poles of the Gauss map g. In other words: the poles of J_F are points on the surface with vertical normal. – The parameter lines on the surface clearly are the image under the Weierstrass integral of the grid on the torus shown before.

The Coordinate Viewpoint

The minimal surface just discussed could have been computed in the described way, but it was not. So far we looked at the torus as a quotient $\mathbb{C}/\Gamma$ and meromorphic functions on a torus therefore were the same as meromorphic functions in $\mathbb{C}$ which had the translations $\tau \in \Gamma$ as periods, meaning $f(z + \tau) = f(z)$. And the Weierstrass integral was evaluated on a fundamental parallelogram for the lattice Γ.

Elliptic functions $J : \mathbb{C}/\Gamma \mapsto \mathbb{C}$ are, away from their branch points, locally invertible. They can therefore be viewed as coordinate functions on the torus. The Weierstrass data of our doubly periodic surface are given in terms of such a function J. We also need to express dz in terms of J, namely: $dz = dJ/J'$. This is almost all what we need, to perform the Weierstrass integration not on the torus, but in the range of the coordinate function J, i.e. in $\mathbb{C}$. We still need to express J' in terms of J. The Jacobi-type elliptic functions which we constructed in 'Symmetries of Elliptic Functions' all had four branch values: $\pm B, \pm 1/B$. The two functions $(J')^2$ and $(J^2 - B^2) \cdot (J^2 - 1/B^2)$ have the same four double zeros and the same two fourth order poles. Since the domain torus is compact this implies that these two functions are proportional. We ignore this multiplicative constant because it only determines the scaling-size of the fundamental domain. Thus we derived the ...

Differential Equation for Jacobi-type Elliptic Functions:

$$J'(z)^2 = P(J) = J^4 - (B^2 + B^{-2}) \cdot J^2 + 1,$$
$$J''(z) = P'(J)/2 = 2J^3 - (B^2 + B^{-2}) \cdot J.$$

And the above Weierstrass data take this form:

$$g(J) = c \cdot J, \ dh = \frac{1}{J} \cdot \frac{dJ}{\sqrt{(P(J))}}, \ J \in \mathbb{C}.$$

This looks much simpler than before and can be directly integrated on a standard polar coordinate grid in $\mathbb{C}$. The remaining problem is the square root. It is a multivalued function and we have to choose the correct branch. Since we are doing path integrals along curves which avoid the branch values (i.e. the zeros of the polynomial P), such an analytic continuation of the square root can be built into the integration routine.
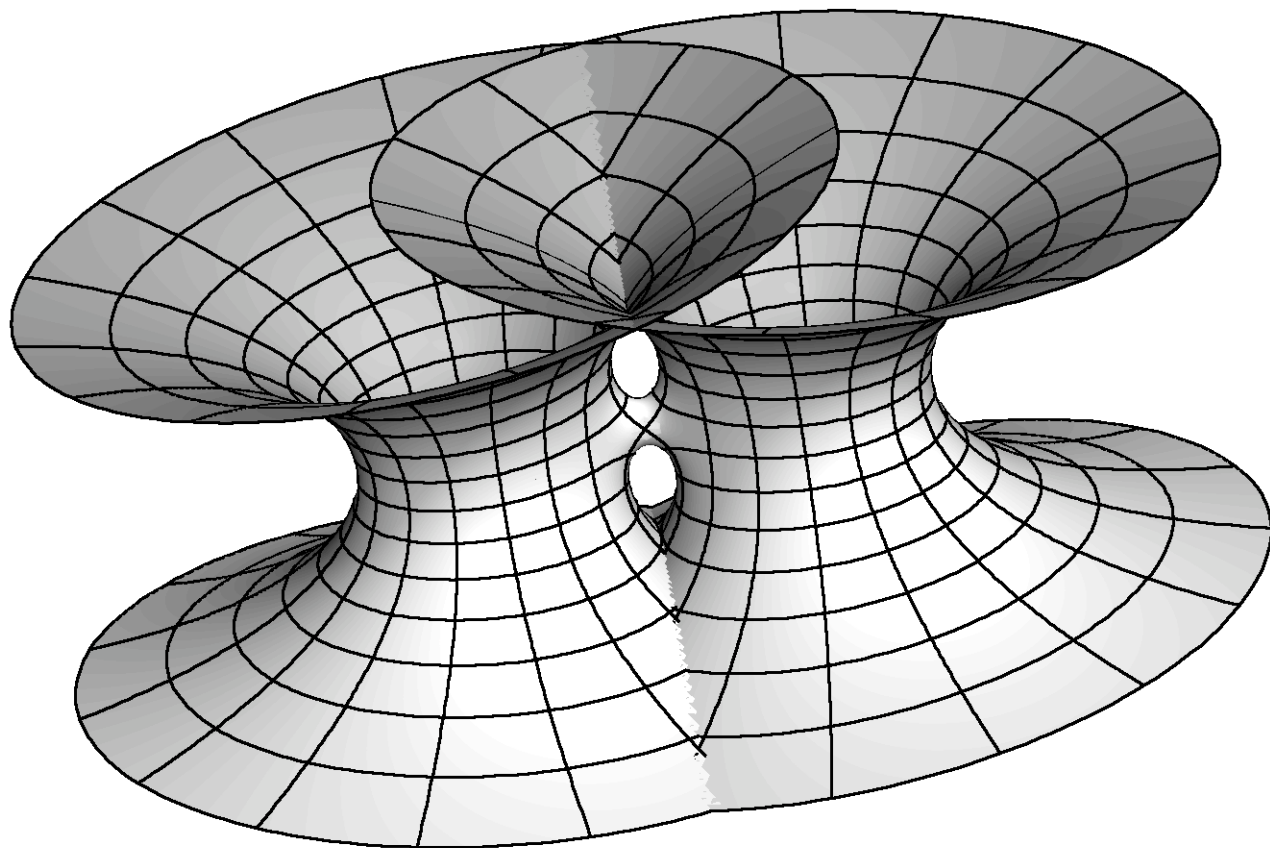
REMARK 1. This coordinate view point is a first important step towards the theory of Riemann surfaces. While for tori this view point is only a simplification, it becomes essential for minimal surfaces parametrized by higher genus surfaces.

REMARK 2. The above differential equation is an example where the dominating Runge-Kutta method fails: If one starts the integration at a zero of P then Runge-Kutta produces a constant solution. There are 4th order methods which use J'' and work fine.
The same is already true for the ODE $(\sin')^2 = 1 - \sin^2$.

Half-Catenoids with opposite normals

How can one find a Weierstrass representation for this surface?

The surface looks like two catenoids joined by a handle, in other words: a sphere with four half-catenoid punctures. We place the surface so that the four limiting normals of the half-catenoids lie in the horizontal plane and form small angles $\pm\varphi$ with the y-axis. On the handle, and also on the waist of each catenoid, one sees one point with the normal pointing vertically up, one point with the normal down. The gauss map therefore has three zeros and three poles on the real axis: $g(z) = z(z^2 - r^2)/(1 - r^2 z^2)$. They are positioned symmetric to the y-axis and to the unit circle. The differential dh must have 6 zeros at these points to

make them into finite points on the surface, and it must have four double poles on the unit circle to create the horizontal half-catenoids. This gives a 2-parameter family of Weierstrass data:

$$g(z) := z \frac{z^2 - r^2}{1 - r^2 z^2},$$

$$dh := (1 - \frac{z^2 + z^{-2}}{r^2 + r^{-2}})(\frac{z^2 + z^{-2}}{e^{2\varphi} + e^{-2\varphi}} - 1)^{-2} \frac{dz}{z}.$$
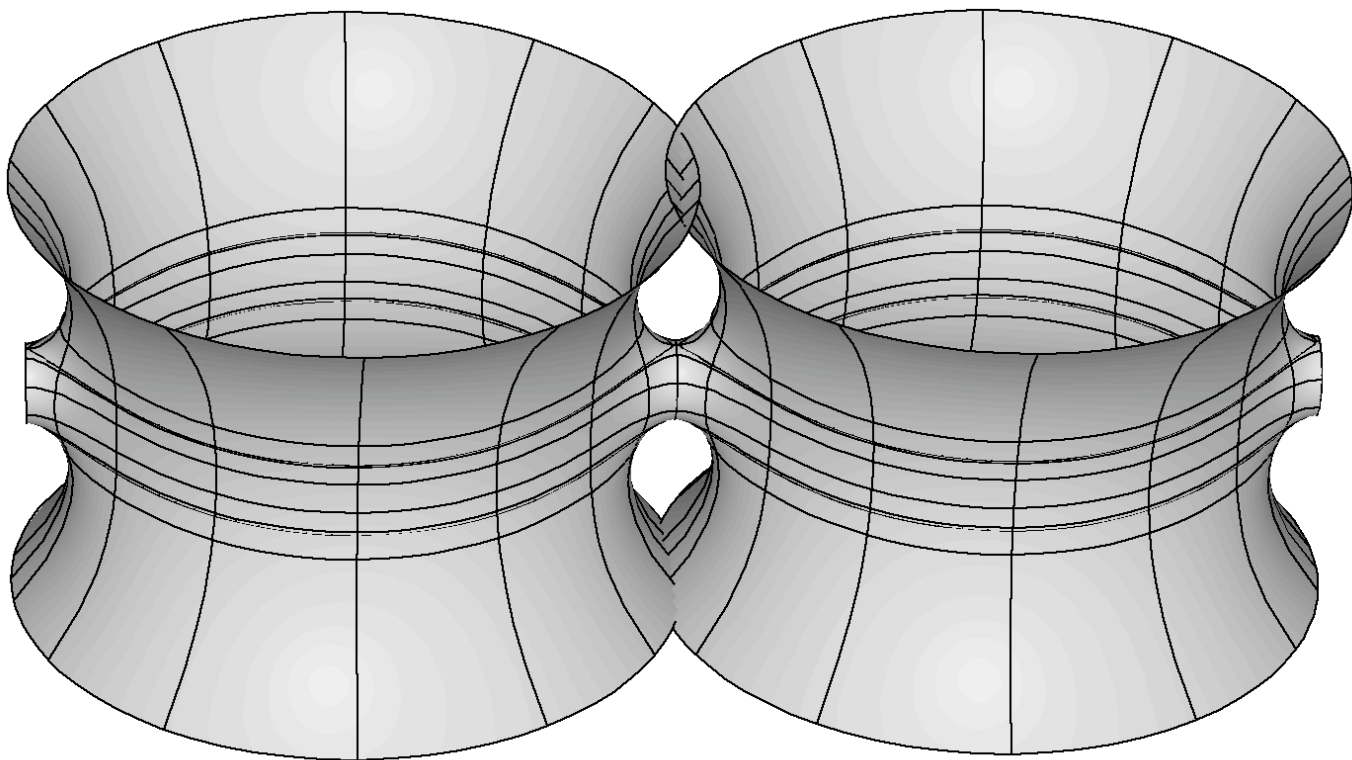
For most choices of parameters the half-catenoid punctures have vertical periods. A residue computation shows that these periods vanish if

$$e^{2\varphi} + e^{-2\varphi} = 2 \cos 2\varphi = 4r^2/(1 + r^4).$$

Historically this is the first surface that showed David Hoffman and me a *handle which connected two minimal surfaces*, deforming them slightly.
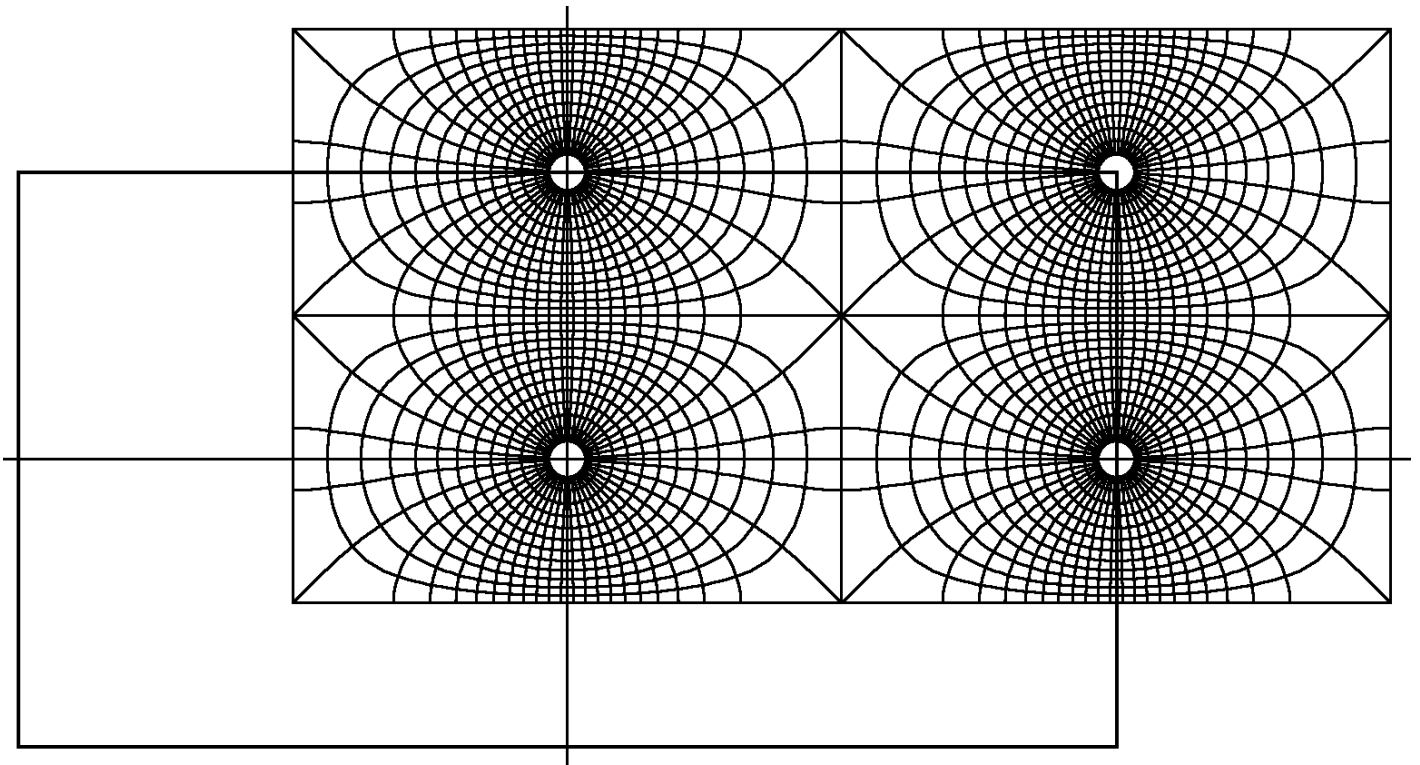
If we imagine such handles to grow in two opposite directions out of the waist of the catenoid, then symmetry would allow the catenoid to stay straight. Therefore we can think of making a *fence of parallel catenoids*, joined by handles. Parallel translation from the symmetry plane of one handle to the symmetry plane of the next handle would be a congruence map of this surface. The quotient by this translation group is a torus with two half-catenoid punctures whose limiting normals point in opposite directions. The handle has two points with normals parallel to the limiting normals of the half-catenoids. The surface in the following picture therefore has a Gauss map with

two zeros and two poles. One zero and one pole are half-catenoid punctures, the other two are finite points on the handle.

So first, what kind of a torus is this? There are two types of tori which have involutive symmetries, the rectangular tori and the rhombic tori. They are easy to distinguish: the fixed point set of such an involution of a rectangular torus has two components, while such involutions of rhombic tori have fixed point sets with only one component. (Note that the interruption of a fixed point set by a puncture is ignored in this count because the puncture is a point on the torus, it is only missing on the image minimal surface.) There are symmetry lines going from the handle into each puncture: They lie in the same plane and are two components of the fixed point set of the surface reflection

in this plane. The parametrizing torus is therefore rectangular. Each of the two symmetry arcs joins points with vertical normals in opposite directions. The following picture allows to visualize this elliptic function, it is again the preimage of a standard polar grid on the Riemann sphere.

The left bottom and right top polar centers are zeros of the function, the other two polar centers are first order poles. Because of this diagonal arrangement this function is called J_D in 'Symmetries of Elliptic Functions'. The rectangles which are filled with a polar grid are preimages of the unit circle. The branch points are the points where more than 2 parameter lines cross. For rectangular tori, the branch values are all on the unit circle.

We will make the two top polar centers the punctures, the two bottom polar centers the finite points with vertical normals (on the handle). Then the function J_F, repre-

sented by the earlier grid, gives us the second part of the Weierstrass data:

$$g(z) := J\_D(z), \ dh := J\_F(z)dz.$$

As before we can integrate in the range of an elliptic function of our choice. The functions J_D, J_F can be computed from each other by solving quadratic equations (D is the branch value of J_D in the first quadrant):

$$J\_D + \frac{1}{J\_D} = \frac{D + 1/D}{2}(J\_F + \frac{1}{J\_F}),$$

$$(J\_F)' = J\_F \cdot (J\_D)'(0) \cdot \left(\frac{1}{J\_D} - J\_D\right),$$

$$dz = d(J\_F)/(J\_F)'.$$

(Recall: $(J\_D)'(0)$ controls the size of the fundamental domain.) Again square roots appear and the correct branch has to be chosen. (For the last surface a more complicated grid than the standard polar grid on the sphere was used.)
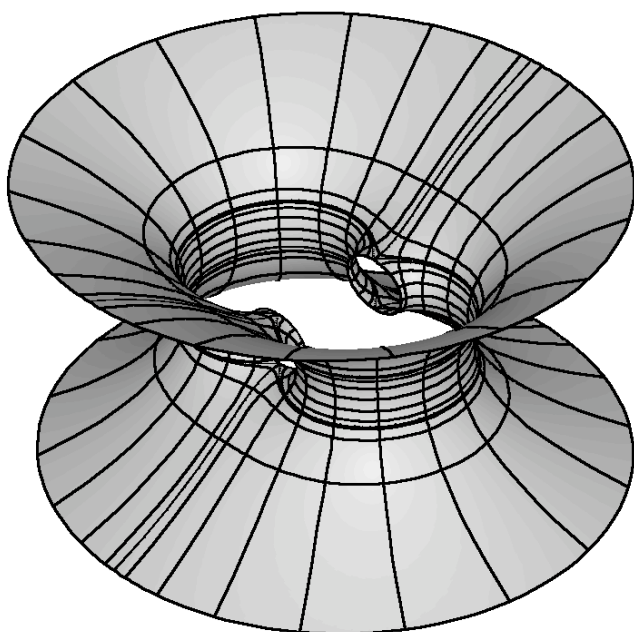
So far we have explained how the Weierstrass representation works for minimal surfaces which are punctured tori. But we have not touched an important question. The Weierstrass representation is well suited to create immersions, and rather many easily. But it requires separate considerations to decide whether the immersed surface is without selfintersections, whether it is *embedded*. For 300 years the plane and the catenoid were the only complete embedded minimal surfaces (CEMS) which have finite to-

tal curvature. Finite total curvature means that the normal Gauss map from the surface to the unit sphere has finite degree, i.e. there is a number d such that almost all points of the sphere are hit d times by the gauss map. Or put differently: that the Gauss map is a meromorphic function.

Lopez-Ros have proved that the only CEMS of finite total curvature *which are conformally punctured spheres*, are the plane and the catenoid.
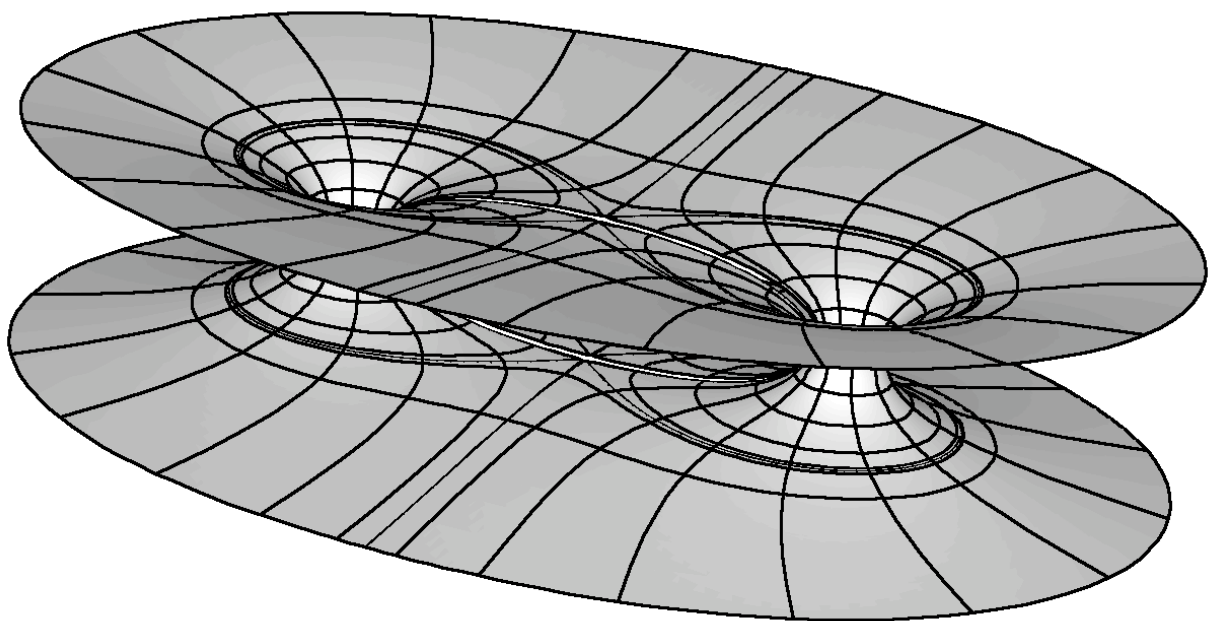
R. Schoen has proved that the only CEMS which have no more infinities than *two catenoid punctures* are the catenoids themselves.

There is an obvious attempt to make a torus with two catenoid ends: Instead of growing handles to the outside - which created the fence of catenoids above - one can grow the handles to the inside. It is easy to start with small handles which are too short to meet in the middle:
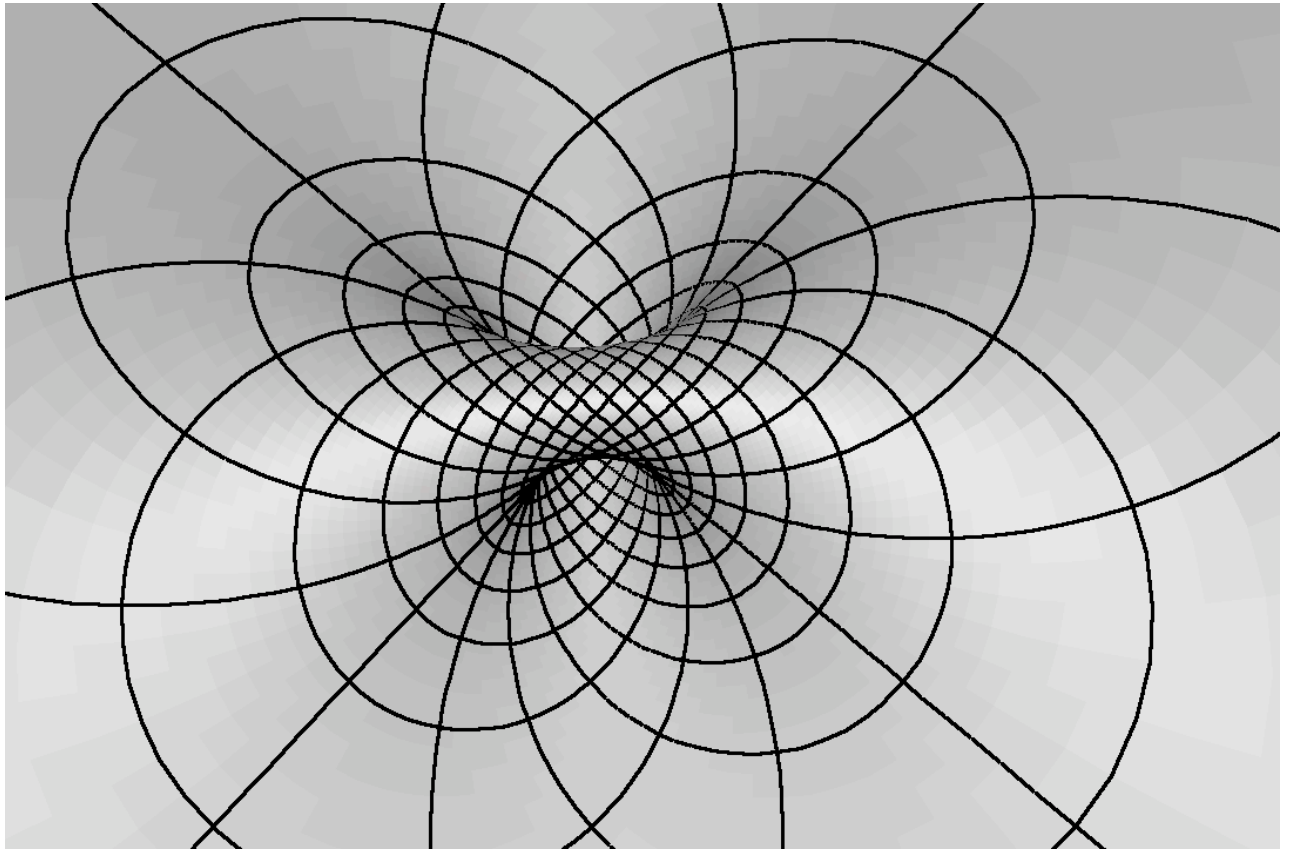

The handles end in planar symmetry lines which - *after translation!* - fit together perfectly. The only problem is that a curve, which is closed on the torus, has a Weierstrass image in $\mathbb{R}^3$ that is not closed, it has a nonzero *period.* Schoen's theorem forbids that one can make the handles long enough. So, how does the example fail?

Things go well for a while: the handle grows and the gap narrows. But, as one changes the parameter further in the promising direction, the mouth of the handle becomes very elongated and the surface starts to look like *two catenoids* whose far out portions are connected. Except that the gap remains no matter how far apart the middle portions of the two catenoids are pushed. The following picture shows how close to a counterexample of Schoen's theorem one gets, or, what difficulties Schoen's proof has to overcome.

Failing attempt to grow a handle through a catenoid.

It was a big surprise when Costa found a minimally immersed punctured torus which Hoffman and Meeks proved to be embedded! The surface is a bit similar to our early example where two half-catenoids grow out of a plane. Therefore we first try to imagine a torus with a planar end. This is a difficult request until one turns it around and asks for a plane with a handle:
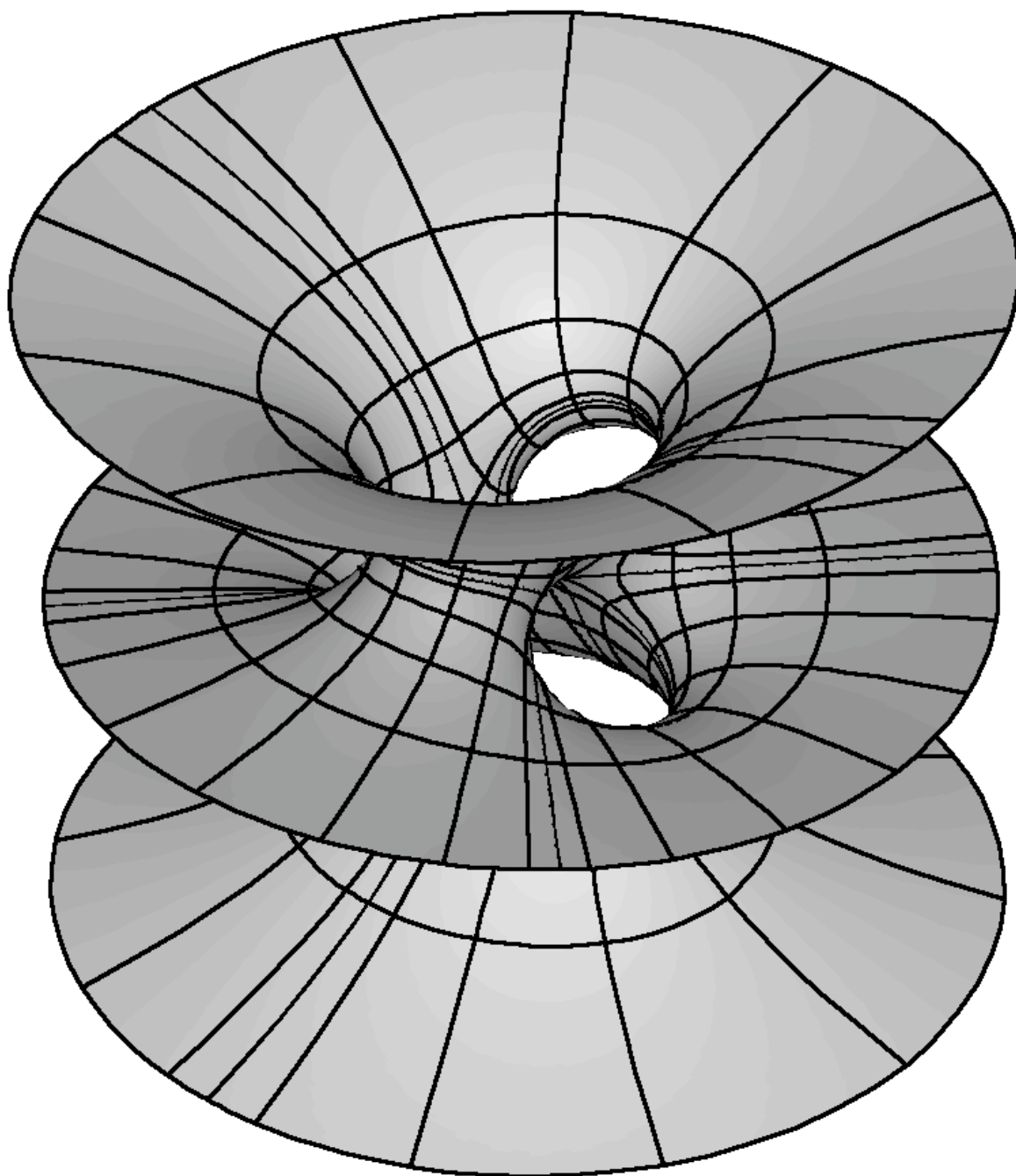
A plane with a handle is *a torus with a planar end.*

This surface is a stereographic projection of the Clifford torus, the projection center is on the surface. All its parameter lines are circles, except for the two straight lines which pass through the midpoint of this surface. It is a torus with one puncture. The torus is the *square torus* because it is a) rectangular since the fixed point sets (on the surface) of the reflections in two vertical planes have *two components* and it is b) rhombic because 180° rotation about the straight lines are symmetries whose fixed point sets have only *one component.*
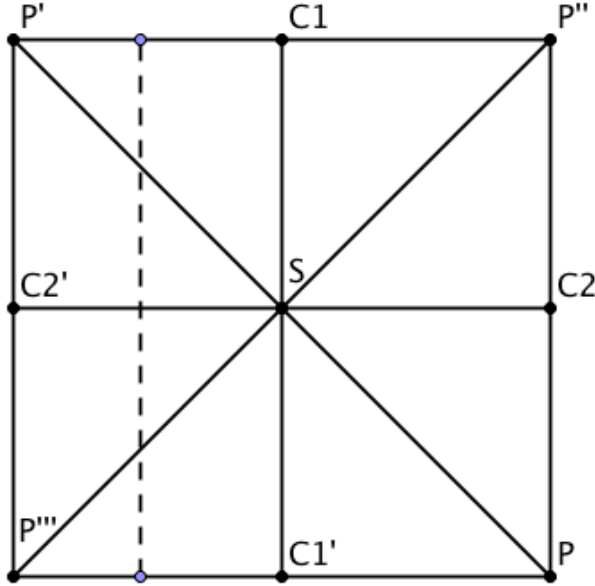
The strategy is: puncture the torus in the two points where the normal to the two straight lines (= the intersection of the symmetry planes) intersect the surface again and grow half-catenoids at these points towards the outside (or away from the straight lines).

This plan contains enough information to write down the Weierstrass data of the

Costa Surface.

We draw the quadratic fundamental domain of our square torus such that the straight lines on the cyclide surface become the diagonals. Note that they are also one component fixed point sets of orientation reversing involutions. The pair of horizontal symmetry lines (the parallel boundary segments are identified) are a two component fixed point set of an involution, and the pair of vertical symmetry lines also. The points $C1, C2$ are the punctures for the half-catenoids. The point P is the (conformal) point at infinity of our plane with handle. The center is called S (for saddle). The normals at $S, C1, C2$ point in one direction, the normal at P in the opposite direction. We take these directions as vertical so that the Gauss map has simple zeros at $S, C1, C2$ and therefore a triple pole at P.

This forces the height differential dh to have simple poles at $C1, C2$ to make these points catenoid punctures. At S we need to compensate the simple pole of $1/g$ with a simple zero. The remaining other simple zero would cause a branch point everywhere except if it is at P. These zeros and poles determine g up to a factor $a \exp(i \cdot \alpha)$ and dh up to a factor $b \exp(i \cdot \beta)$. Clearly b only scales the surface and α rotates it. And β is the associate family parameter, it is chosen to make the pe-

riods of the catenoid punctures imaginary. Under these conditions the fixed point sets of the involutions turn out to be straight lines (the diagonals) and planar geodesics. This was not at all clear initially, but it follows immediately from the description of the functions in 'Symmetries of Elliptic Functions'. With the parameter a we have at this point the Weierstrass data of a 1-parameter family of candidates. With an intermediate value argument one can choose a so that the dotted curve - which is closed on the torus - also has a closed Weierstrass image in $\mathbb{R}^3$.

Weierstrass Data for the Costa Surface:

$$g(z) = a \cdot (J\_E \cdot J\_F)'(z), \ dh = \frac{dz}{J\_D(z)}.$$

Up to a multipicative constant the function $J\_E \cdot J\_F$ is the Weierstrass $\wp$-function (here for the square torus).

The Conjugate Plateau Construction
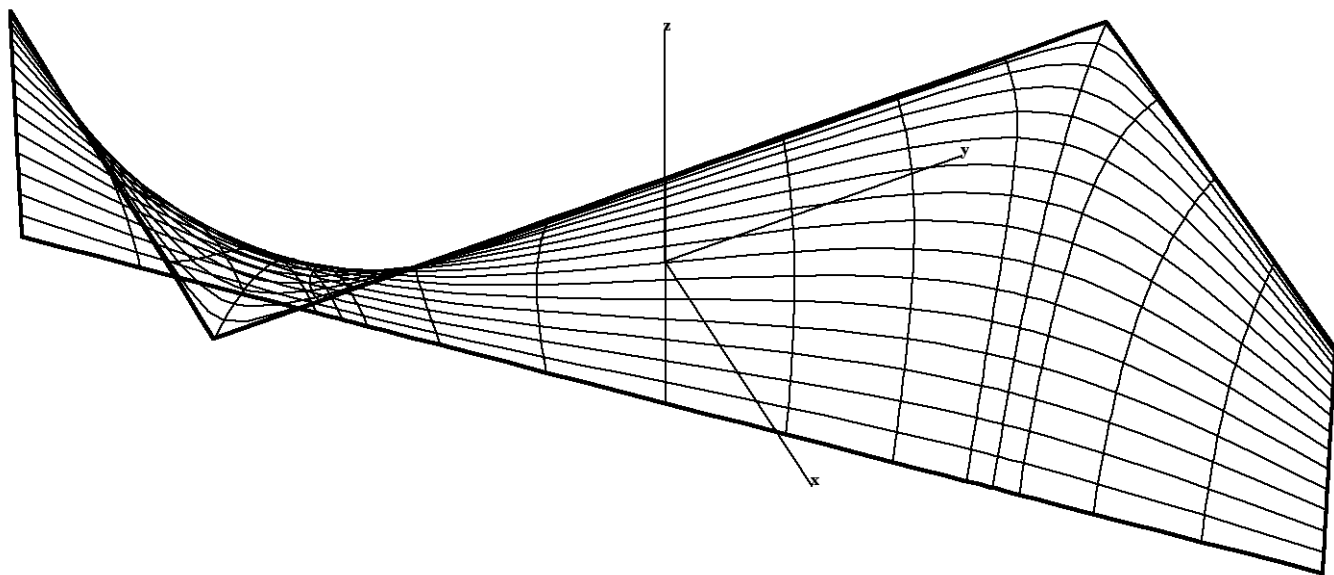# Of Triply Periodic Minimal Surfaces

The Weierstrass representation for triply periodic minimal surfaces is more difficult than what we have explained so far. A simpler approach is the *conjugate Plateau construction* which, as we will see, can loosely be called the soap film point of view. Without further explanation we use the fact from complex analysis that the derivative of the imaginary part of a function $z \mapsto f(z)$ can easily be computed from the derivative of the real part of f. This fact is known as the 'Cauchy-Riemann equations'. It implies that, on a simply connected domain, the real part of f determines the imaginary part up to a constant. Of course this holds for the three components of the Weierstrass integral so that a simply connected minimal surface piece determines its conjugate surface up to an $\mathbb{R}^3$-constant.

The next step is the soap film part: The Plateau problem arose from the soap film experiments of the 19th century physicist Joseph A. F. Plateau. Its solution (1932) by Douglas and Rado states:
Every closed continuous injective curve in $\mathbb{R}^3$ is the boundary of at least one simply connected minimal surface.
This theorem expresses a fundamental property of the minimal surface equation: It is well suited for boundary value problems. On the other hand, initial value problems usually have no solution. In particular, the minimal surface piece of a Plateau solution usually cannot be extended beyond its boundary curve. So, how can it help to get complete solutions without boundary?

Here symmetries come to the rescue. If the boundary curve contains a straight line segment then 180° rotation of a Plateau solution around this segment extends the minimal surface to twice as large a piece. If the boundary curve is a polygon then extension by 180° rotation works for all segments of the original polygon and all segments of the rotated polygons. The resulting surfaces usually have singularities at the vertices of these polygons. However, if all the angles of the polygon are of the form $\pi/k, k \in \mathbb{N}$, then repeated rotation about the edges that start at one vertex p results in a surface for which p is an interior, regular point. Such contours therefore lead to complete minimal surfaces without boundary, but usually with lots of self-intersections. Only a few such minimal surfaces, which are embedded, are known. An example is the conjugate of the Schwarz' P-surface:

All angles of this hexagon are 90°, the z-axis divides it into two 90°-pentagons.

The next step gives us a wealth of embedded examples. We consider the conjugates of the just described Plateau solutions with polygonal boundaries. A surprise happens to the straight line segments of the boundary which are symmetry lines on the extended surface with the symmetry being 180°-rotation:

The boundary of the conjugate piece consists also of symmetry arcs. These arcs are planar geodesics and the extended surface is reflection symmetric with respect to these planes.
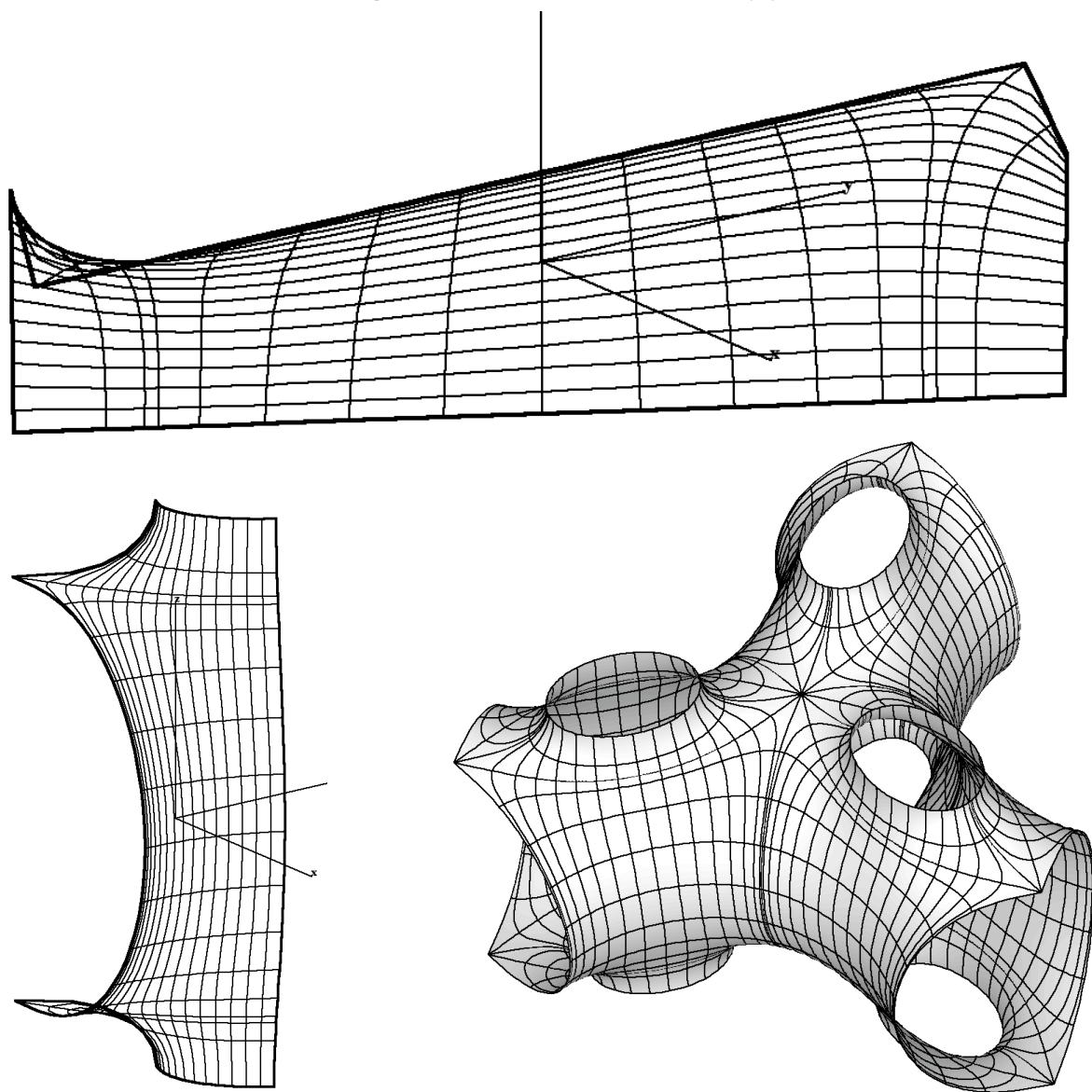
The strategy of the conjugate Plateau construction is, to choose the polygonal contour for the Plateau solution in such a way that the extension of its conjugate piece by reflection in the planes of the boundary arcs give an embedded minimal surface.

This is helped by two geometric facts:

(i) The Plateau solution very often is a graph over a convex domain which is bounded by a suitable orthogonal projection of the boundary polygon. Therefore it is embedded. Romain Krust proved that in this situation the conjugate piece is also a graph, hence embedded.

(ii) The boundary polygon determines the angle by which the normal of the Plateau solution rotates along each boundary segment. The Weierstrass representation shows that the normal of the conjugate piece rotates along each boundary arc by *the same angle.*

The Fujimori-Weber surfaces are very good examples for the described construction. In the Action Menu one can

select `Don't Show Reflections` to see the fundamental piece. Also in the Action Menu one can switch between a minimal surface and its conjugate. In the View Menu one can switch between `WireFrame Display`, `Patch Display`, `Point Cloud Display`. In WireFrame and in Point Cloud Display the Action Menu offers `Emphasize Boundary`, so that one can easily see the polygonal contour for the Plateau solution and its conjugate – which is the fundamental piece of a Fujimori-Weber surface, bounded by planar symmetry arcs. The following pictures are an $ff = 4$ example:

The Plateau contour is a hexagon with four 90° and two 60° angles. The z-axis divides it into two pentagons. Observe that the conjugate piece has its normals *parallel* to the normals of the Plateau piece – at corresponding points of course. The third picture is an assembly of twelve such fundamental domains.

All of our Fujimori-Weber surfaces can be described in the above way. Note that not only the angles of the hexagon between adjacent edges are important, but also the following: Let a, b, c be three consecutive edges. The angle between a plane normal to a and a plane normal to c has to be either 0 or of the form π/k, $k = 2, 3, 4, 6$. Otherwise the group generated by the reflections in the symmetry planes of the conjugate of the Plateau solution is not discrete and the extended surface cannot be embedded.

Several of the Fujimori-Weber surfaces agree with other examples in 3D-XplorMath: $ff = 2$ is the Schwarz P-surface, $ff = 5$ is the Schwarz H-surface, $ff = 8$ is the A. Schoen S-S-surface and $ff = 7$ is the same surface 'inside-out', that is, the assembled piece has the *other side* of the surface as its outside. If a minimal surface carries a straight line, then the 180° symmetry rotation interchanges the two sides of the surface – therefore there is no geometric distinction between the two sides. Here this happens if the pentagon-half of the Plateau hexagon has a reflection symmetry, as in the cases $ff = 2, 5$ above. The other cases come in such 'inside-out' pairs, which look like different surfaces, but are not, because the pentagon-halfs of the

Plateau hexagon are *the same* polygon. The other pairs are

$ff = 1, 3$ (A. Schoen's H-T–surface),
$ff = 4, 6$ (A. Schoen's H-R–surface) and
$ff = 9, 10$ (A. Schoen's T-R–surface).

Although the triply periodic surfaces in 3D-XplorMath can most easily be understood by this conjugate Plateau construction, they are not computed in this way. It is another story to explain the functions and their domains which are used in the Weierstrass representation to compute these surfaces.

In [Ka] a Weierstrass representation for several Plateau problems as above is derived. Also fifteen 1-parameter polygonal contours are discussed which give further examples because the obstructing period problem can be solved by the intermediate value theorem.

In [FW] the Fujimori-Weber surfaces are obtained with a non-standard use of the Weierstrass representation. The collection of examples described in this paper is much larger than what is shown in 3D-XplorMath.

Bibliography

[Ka] Karcher, H.: The triply Periodic Minimal Surfaces of Alan Schoen And Their Constant Mean Curvature Companions. Manuscripta Math. 64, 291-357 (1989).

[FW] Fujimori S., Weber M.: Triply Periodic Minimal Surfaces Bounded By Vertical Symmetry Planes. Manuscripta Math. 129, 29 - 53 (2009).